RSC Advances

PAPER

View Article Online
View Journal | View Issue

Cite this: *RSC Adv.*, 2023, **13**, 32150

Synthesis and biological evaluation of capsaicin analogues as antioxidant and neuroprotective agents†

Mao Xie,‡[a] Huixian Wu,‡[ab] Jing Bian,‡[c] Shutong Huang,[b] Yuanzheng Xia,[c] Yujun Qin[c] and Zhiming Yan *[ab]

Received 28th July 2023
Accepted 26th October 2023

DOI: 10.1039/d3ra05107b

rsc.li/rsc-advances

Capsaicin and its analogues **3a–3q** were designed and synthesized as potential new antioxidant and neuroprotective agents. Many analogues exhibited good antioxidant effects, and some showed more potent free radical scavenging activities than the positive drug quercetin (IC_{50} = 8.70 ± 1.75 μM for DPPH assay and 13.85 ± 2.87 μM for ABTS assay, respectively). The phenolic hydroxyl of capsaicin analogues was critical in determining antioxidant activity. Among these compounds, **3k** displayed the most potent antioxidant activity. Cell vitality tests revealed that the representative compound **3k** was good at protecting cells from H_2O_2-induced oxidative damage at low concentrations (cell viability increased to 90.0 ± 5.5% at 10 μM). In addition, the study demonstrated that **3k** could reduce intracellular ROS accumulation and increase GSH levels to prevent H_2O_2-induced oxidative stress in SY5Y cells. In the mitochondrial membrane potential assay, **3k** significantly increased the MMP level of SY5Y cells treated with H_2O_2 and played an anti-neuronal cell death role. These results provide a promising strategy to develop novel capsaicin analogues as potential antioxidant and neuroprotective agents.

1. Introduction

The capsicum genus consists of more than 200 varieties, classified according to the Scoville 'Heat' Units from the very hot habanero to the sweet bell pepper.[1] The spicy ingredients in pepper mainly come from capsaicin (8-methyl-*N*-vanillaldehyde-6-nononic acid) and dihydrocapsaicin, nordihydrocapsaicin, homodihydrocapsaicin, and homocapsaicin, *etc.*, collectively referred to as capsaicinoids.[2] Capsaicinoids are not only widely used as food additives but also used to treat rheumatoid arthritis, post-operative pain, acute/chronic neuropathic and musculoskeletal pain, prostate cancer, leukemia, *etc.*[3] More than two hundred clinical trials were carried out on capsaicin, and most of these focus on the pain-relieving effect of capsaicin.[4] The three structural features of capsaicin are the key to receptor action, including the lipophilic moiety (nonenyl of capsaicin), which can be substituted by the alkyl/alkenyl chain; the polar head (3-methoxy-4-hydroxybenzyl) and the linker (an amide of capsaicin).[5] Kogure *et al.*[6] suggested that the phenolic hydroxyl of capsaicin was not associated with radical scavenging, arguing that the radical scavenging site was the C7-benzyl carbon, and the presence of an acetamide was of great significance for the radicals to obtain hydrogen from the C7-benzyl carbon of capsaicin. On the contrary, Okada *et al.*[7] reported that the radical scavenging site of capsaicin was not dependent on C7-benzyl carbon and acetamide but on the phenolic hydroxyl group of capsaicin, and suggested that the antioxidant site of capsaicin was 2-methoxy-4-methyl-phenol. Capsaicin was a promising small molecule for further optimization.[8–10] Moreover, the role of capsaicin analogues in the structure–activity relationship of anti-oxidative and neuroprotective has not been reported.

In vivo, radicals can be generated through normal physiological reactions. A free radical is a kind of substance that contains one or more lone electrons. Due to the incomplete electron shell, it has high reactivity and participates in various physiological reactions.[11] Reactive oxygen species (ROS) is the active form of oxygen, mainly including oxygen-containing radicals and peroxides prone to the formation of radicals, such as hydrogen (H_2O_2), superoxide (O^{2-}), hydroxyl radical ($^{\bullet}OH$), *etc.*[12] Oxygen participates in high-energy electron transfer and generates large amounts of ATP through oxidative phosphorylation to provide energy in normal physiological

[a]*Department of Otolaryngology-Head & Neck Surgery, First Affiliated Hospital of Guangxi Medical University, Nanning, Guangxi, China*

[b]*Pharmaceutical College, Guangxi Medical University, Nanning, Guangxi, China. E-mail: zhiming_yan@126.com*

[c]*Jiangsu Key Laboratory of Bioactive Natural Product Research, State Key Laboratory of Natural Medicines, School of Traditional Chinese Pharmacy, China Pharmaceutical University, Nanjing, Jiangsu, China*

† Electronic supplementary information (ESI) available: Experimental procedures including characterization data of novel synthetic compounds. See DOI: https://doi.org/10.1039/d3ra05107b

‡ These authors contributed equally to this work.

reactions.[13] Also, the organism is also under oxidative attack by ROS constantly. There are a variety of antioxidant enzymes, such as catalase (CAT), superoxide dismutase (SOD), glutathione peroxidase (GSH-Px), *etc.* ROS produced in cells are continuously cleared by these enzymes, under normal physiological conditions, keeping the organism in a stable oxidation–reduction system balance.[14] Oxidative stress occurs because of an imbalance between ROS production and the ability of the body to counteract its effects.[15] High concentrations of ROS, including hydroxyl, hydrogen peroxide and superoxide, may cause damage to lipids, proteins and DNA of biological system,[16] leading to tissue damage and the development of cataracts, cardiovascular disease, chronic obstructive pulmonary diseases, chronic kidney disease, neurodegenerative diseases, cancer, diabetes and sarcopenia.[17–19]

Neurodegenerative diseases are considered related to the loss of neurons, or their myelin sheaths, they worsen over time and dysfunctional.[20] Oxidative stress is closely related to the occurrence and progression of neurodegenerative diseases, including Parkinson's disease, Alzheimer's disease,[21,22] Huntington's disease and amyotrophic lateralizing sclerosis.[23] The brain has high oxygen consumption and produces a large amount of ROS. Although the brain has an antioxidant defense mechanism, it is mainly composed of glutathione, vitamin E, melatonin and antioxidant enzyme, and its antioxidant capacity is very limited, so the brain is more vulnerable to oxidative damage than other tissues.[24,25] Therefore, antioxidants may be beneficial for neurodegenerative diseases.

ROS are mainly originated from mitochondria, while ROS accumulation further damages mitochondria.[26] Mitochondria are the key factors that determine cell survival and death. Studies suggest the participation of mitochondria dysfunction in neurodegenerative diseases. In addition, excessive ROS can reduce mitochondrial membrane potential (MMP) and then induce cell apoptosis.[27] Thus, increased MMP may rescue and reverse ROS-promoted neuronal cell death and combat neurodegenerative diseases.

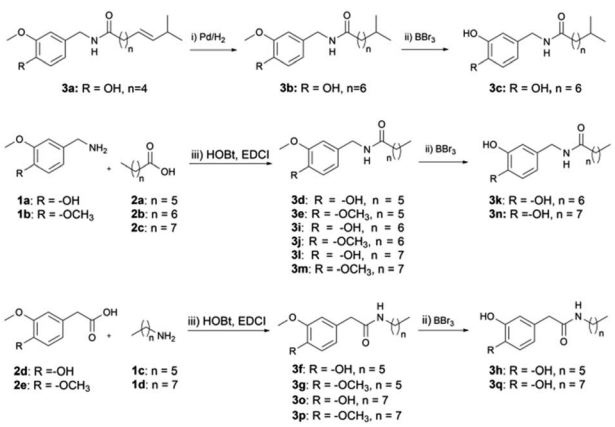

Scheme 1 Synthesis of compounds **3b–3q**. Reagents and conditions: (i) Pd, H_2, THF, r.t., 12–24 h; (ii) BBr_3, −78 °C → r.t., DCM, 4–5 h; (iii) HOBt, EDCI, Et_3N, DCM, r.t., 4–5 h.

In this study, we modified the structure of capsaicin, the main active ingredient of pepper, synthesized a series of capsaicin analogues, and evaluated their antioxidant activity and underlying neuroprotective mechanism.

2. Results and discussion

2.1. Synthesis

Capsaicin analogues were synthesized as shown in Scheme 1. The initial compounds **3a**, **1** and **2** were purchased from the market. Dihydrocapsaicin **3b** could be obtained by hydrogenation from capsaicin **3a**, the amidation of acid **2** and amine **1** generated the intermediates **3d–3g**, **3i–3j**, **3l–3m** and **3o–3p** in the presence of HOBt, EDCI. Finally, the target compound **3c**, **3k**, **3n**, **3h** and **3q** was formed *via* demethylation from the corresponding precursors **3** under BBr_3.

2.2. Prediction of physical properties and BBB penetration of compounds 3a–3q

A major impediment to the development of neuroprotective agents for neurodegenerative diseases is that many large-molecule drugs fail to cross the BBB.[28] Lipinski's rules were used for the prediction of physical properties and BBB penetration of compounds **3a–3q**. Lipinski's rules: molecular weight (MW) ≤ 500, the calculated logarithm of the octanol–water partition coefficient (Clog *P*) ≤ 5, the number of hydrogen bond acceptor atoms (HBA) ≤ 10, the number of hydrogen bond donor atoms (HBD) ≤ 5, and the small polar surface area ≤ 90 Å^2. The calculation of log BB by means of the equation is shown in the footnote of Table 1. As shown in Table 1, compounds **3a–3q** fulfill drug-like criteria and could penetrate the blood–brain barrier.

Table 1 Physical properties compounds **3a–3q**

Compd	MW[a]	Clog *P*[a]	HBA[a]	HBD[a]	tPSA[a]	log BB[a]
3a	305.41	3.43	3	2	58.56	−0.22
3b	307.43	3.7	3	2	58.56	−0.17
3c	293.4	3.34	3	3	69.56	−0.39
3d	265.35	2.73	3	2	58.56	−0.32
3e	279.37	3.13	3	1	47.56	−0.10
3f	265.35	2.67	3	2	58.56	−0.33
3g	279.37	3.07	3	1	47.56	−0.11
3h	251.32	2.44	3	3	69.56	−0.53
3i	279.37	2.42	3	2	58.56	−0.37
3j	293.4	3.51	3	1	47.56	−0.04
3k	265.35	2.82	3	3	69.56	−0.47
3l	293.4	3.44	3	2	58.56	−0.21
3m	307.43	3.82	3	1	47.56	0.01
3n	279.37	3.12	3	3	69.56	−0.43
3o	293.4	3.38	3	2	58.56	−0.22
3p	307.43	3.84	3	1	47.56	0.01
3q	279.37	3.16	3	3	69.56	−0.42
Rules	≤500	≤5.0	≤10	≤5	≤90	≥−1.0

[a] MW: molecular weight, Clog *P*: calculated logarithm of the octanol–water partition coefficient, HBA: hydrogen-bond acceptor atoms, HBD: hydrogen-bond donor atoms, tPSA: polar surface area, log BB = −0.0148 × tPSA + 0.152 × Clog *P* + 0.130.

Table 2 Antioxidant activity of compounds **3a–3q**

Compd	R	*n*	DPPH[a] (IC_{50}, μM)	ABTS[b] (IC_{50}, μM)
3a	–OH	4	52.07 ± 3.21	16.89 ± 1.64
3b	–OH	6	50.87 ± 4.08	11.26 ± 1.55
3c	–OH	6	7.33 ± 0.98	16.77 ± 2.10
3d	–OH	5	67.64 ± 4.74	24.32 ± 3.62
3e	$-OCH_3$	5	27.33 ± 2.88%[c]	11.47 ± 2.47%[c]
3f	–OH	5	138.72 ± 6.89	13.07 ± 1.47
3g	$-OCH_3$	5	12.76 ± 2.54%[c]	12.45 ± 1.03%[c]
3h	–OH	5	4.49 ± 0.74	18.60 ± 3.03
3i	–OH	6	27.89 ± 4.55	13.61 ± 2.90
3j	$-OCH_3$	6	22.72 ± 5.47%[c]	11.73 ± 3.11%[c]
3k	–OH	6	5.06 ± 1.34	10.62 ± 1.28
3l	–OH	7	27.20 ± 3.47	44.16 ± 4.65
3m	$-OCH_3$	7	18.56 ± 2.33%[c]	8.06 ± 1.17%[c]
3n	–OH	7	5.91 ± 0.77	22.66 ± 2.34
3o	–OH	7	184.93 ± 9.86	30.88 ± 2.79
3p	$-OCH_3$	7	30.48 ± 3.44%[c]	20.08 ± 3.22%[c]
3q	–OH	7	4.14 ± 1.09	21.64 ± 3.69
Quercetin	—	—	8.70 ± 1.75	13.85 ± 2.87

[a] IC_{50} values were expressed as mean ± SEM for three determinations. [b] Data were expressed as IC_{50}, the compound's concentration that inhibits 50% of free radicals (mean ± SEM). [c] The measurements were performed in the presence of 0.5 mM compounds.

2.3. Antioxidant activity

2.3.1 General. Alam *et al.* reported a variety of methods for determining the antioxidant activity of compounds *in vitro*.[29] In this study, DPPH free radical scavenging activity assay and ABTS radical cationic decolorization assay were used to evaluate the radical scavenging ability of 17 compounds (**3a–3q**) to determine their antioxidant activities.

2.3.2 Antioxidant activity determined by DPPH radical scavenging assay. The reduction of oxidative stress was a crucial aspect in finding food ingredients for the prevention and treatment of neurodegenerative diseases or others. The antioxidant activity of capsaicin analogues **3a–3q** was tested by DPPH radical scavenging assay using quercetin as a reference compound. Most of the analogues exhibited potent free radical scavenging activities. The IC_{50} values or inhibiting rates of all capsaicin analogues were summarized in Table 2. From the table, compounds **3c**, **3h**, **3k**, **3n** and **3q** showed more potent (IC_{50} = 7.33 ± 0.98 μM, 4.49 ± 0.74 μM, 5.06 ± 1.34 μM, 5.91 ± 0.77 μM and 4.14 ± 1.09 μM, respectively) than the reference compound quercetin (IC_{50} = 8.70 ± 1.75 μM), while compounds **3e**, **3g**, **3j**, **3m** and **3p** had little radical scavenging activities. These studies showed that dual –OH groups were critical in determining scavenging activity and dual $-OCH_3$ groups were unfavorable for antioxidant activities. For example, compound **3c** (IC_{50} = 7.33 ± 0.98 μM) derived from the demethylated dihydrocapsaicin **3b** (IC_{50} = 50.87 ± 4.08 μM) showed increased potent scavenging activity. Compounds **3d**, **3f**, **3i**, **3l** and **3o** respectively derived from the demethylated compounds **3e**, **3g**, **3j**, **3m** and **3p** had increased antioxidant activities. Compounds **3h**, **3k**, **3n** and **3q** (IC_{50} = 4.49 ± 0.74 μM, 5.06 ± 1.34 μM, 5.91 ± 0.77 μM and 4.14 ± 1.09 μM, respectively) with two –OH groups showed more potent scavenging activities than the compounds **3f**, **3i**, **3l** and **3o** (IC_{50} = 138.72 ± 6.89 μM, 27.89 ± 4.55 μM, 27.20 ± 3.47 μM and 184.93 ± 9.86 μM, respectively) with one –OH and $-OCH_3$ groups. Besides, from the antioxidant values and amide structure comparison of compounds (**3d** *vs.* **3f**, **3e** *vs.* **3g**, **3l** *vs.* **3o**, **3m** *vs.* **3p**, **3n** *vs.* **3q**), it appeared that the structural sequence of amides seems to be little influence to scavenging activity. IC_{50} values or inhibiting rates of different compounds (**3a** *vs.* **3b**, **3d** *vs.* **3i** *vs.* **3l**, **3e** *vs.* **3j** *vs.* **3m**, **3h** *vs.* **3k** *vs.* **3n**, **3f** *vs.* **3o**, **3g** *vs.* **3p** and **3h** *vs.* **3q**) indicated that no matter whether the length of alkyl chain or alkenyl chain was contributed relatively less to the DPPH-scavenging. In brief, the capsaicin analogues antioxidant effects of the structure–activity relationship were as follows: two –OH groups on the benzene ring > one –OH and one $-OCH_3$ groups on the same benzene ring > two $-OCH_3$ groups on the same benzene ring.

2.3.3 Antioxidant capacity determined by ABTS radical cationic decolorization assay. These capsaicin analogues tested for their radical scavenging activities (DPPH) were also tested for radical cationic decolorization assay (ABTS). The antioxidant effects were shown as IC_{50} values and quercetin was used as a reference compound. The IC_{50} values or inhibition ratio of these compounds were summarized in Table 1. Most of the compounds showed good radical scavenging ability the IC_{50} values ranging from 10.62 μM to 44.16 μM. Compound **3f**, **3i** and **3k** showed significant antioxidant activity (IC_{50} = 13.07 ± 1.47 μM, 13.61 ± 2.90 μM and 10.62 ± 1.28 μM respectively). As can be seen from Table 2, when the two substituents on the benzene ring are methoxyl (**3e**, **3g**, **3j**, **3m** and **3p**), $ABTS^+$ radical scavenging rate does not exceed 20% at 0.5 mM concentration, and the antioxidant effect is consistent with the result of DPPH radical scavenging assay. Unlike the structure–activity relationship for the DPPH assay, compounds with two –OH groups (**3c**, **3h**, **3k**, **3n** and **3q**) have similar antioxidant effects to compounds with one –OH and one $-OCH_3$ groups (**3b**, **3f**, **3i**, **3l** and **3o**). In addition, compound **3k** (IC_{50} = 10.62 ± 1.28 μM) showed the best antioxidant capacity and was significantly better than the standard reference control quercetin (IC_{50} = 13.85 ± 2.87 μM). In a word, the capsaicin analogues antioxidant (ABTS assay) effects of the structure–activity relationship were as follows: two –OH groups on the benzene ring ≈ one –OH and one $-OCH_3$ groups on the same benzene ring > two $-OCH_3$ groups on the same benzene ring.

2.4. 3k protected SH-SY5Y cells from H_2O_2

Many studies have shown that oxidative stress is an important cause of neurodegenerative diseases.[30] However, this non-equilibrium state is produced by cells overproducing ROS, which exceeds the scavenging capacity of their antioxidant system. ROS can react with different molecules to promote neuronal cell death and cause neurodegenerative diseases.[31,32] H_2O_2 is one of the ROS produced by metabolism *in vivo* and is often used to establish an *in vitro* oxidative stress model.[33] Firstly, compounds **3a**, **3b**, **3c**, **3k**, **3n**, **3q** and quercetin were tested for cytotoxicity by MTT assay respectively. As shown in Fig. 1A, compounds **3c**, **3n**, or **3q** displayed strong growth inhibition on SH-SY5Y cells. Therefore, compounds **3a**, **3b**, **3k**

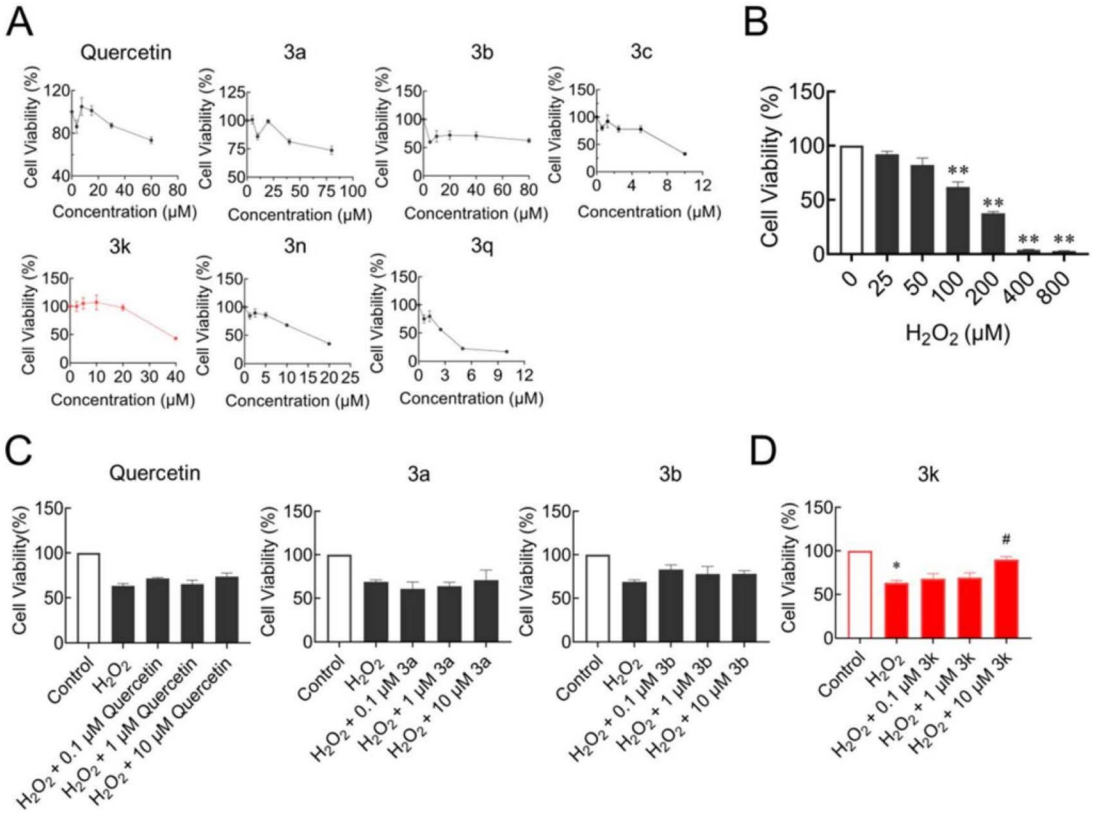

Fig. 1 **3k** markedly enhanced SH-SY5Y cell viability induced by H_2O_2. (A) Cytotoxicity of compounds **3a**, **3b**, **3c**, **3k**, **3n**, **3q** and quercetin. (B) Screening of H_2O_2 concentration with MTT assay. (C and D) MTT assay of SH-SY5Y cells exposed to 100 μM H_2O_2 with or without **3a**, **3b**, **3k** or quercetin preincubation. The absorbance of control cells was regarded as 100%. Error bars represented SEM. *P < 0.05, and **P < 0.01, *versus* control. $^{\#}P$ < 0.05 *versus* 100 μM H_2O_2 treated group.

and quercetin were selected for further detection. To establish the oxidative stress model, the cell viability of SH-SY5Y in the presence of 25–800 μM H_2O_2 was tested by MTT assay. H_2O_2 at the concentrations of 25 and 50 μM had no apparent inhibitory or promotive effects on SH-SY5Y cells (Fig. 1B). While with the increase of the concentration of H_2O_2, SH-SY5Y cell viability gradually decreased in a concentration-dependent manner. H_2O_2 at 100 μM showed 38.1 ± 7.6% inhibition in SH-SY5Y cells, thus 100 μM H_2O_2 was chosen for further experiments (Fig. 1B).

Then, the capacity to resist oxidative stress of four compounds **3a**, **3b**, **3k** or quercetin were investigated respectively. Compared with the control, the cell viability of H_2O_2-treated SY5Y cells decreased to 63.3 ± 4.5%, which proved that the oxidative stress model was stable and repeatable (Fig. 1C). Chemicals at the concentration of 0.1 μM, 1 μM or 10 μM were pretreatment respectively. Compound **3k** showed antioxidative capacity, and the cell viability increased dose-dependently manner. Significantly, **3k** at 10 μM increased the cell viability to 90.0 ± 5.5% (Fig. 1D).

2.5. 3k reduced the accumulation of intracellular ROS and enhanced the antioxidative capacity of SH-SY5Y cells

To detect whether **3k** suppressed cell death *via* decreasing oxidative stress, the intracellular ROS levels of SY5Y cells were measured by using DCFH-DA assay. The intensity of fluorescence generally represents the degree of oxidation. The results showed that the green fluorescence intensity of cells was significantly enhanced after 24 h treated with H_2O_2 compared with control, which indicated the ROS levels were elevated (Fig. 2A). The fluorescence intensity was decreased gradually with concentration gradient **3k** treatment. These results demonstrated **3k** inhibited the degree of oxidation and protected SY5Y cells from oxidative stress. In addition, we examined GSH, which plays a significant role in protecting oxidative

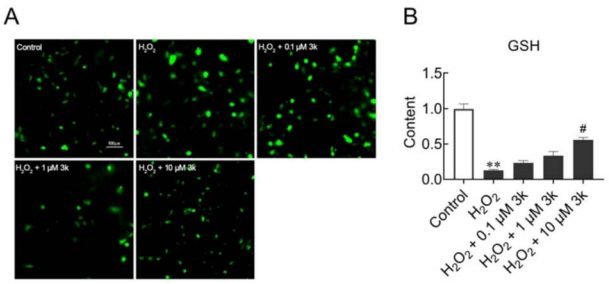

Fig. 2 **3k** inhibited ROS levels and increased GSH content in H_2O_2-injured SY5Y cells. (A) **3k** restrained the overproduction of intracellular ROS. DCFH-DA probe was used to detect ROS fluorescence intensity. (B) **3k** improved GSH levels. Error bars represent SEM. $^{\#\#}P$ < 0.01 *versus* control. *P < 0.05 *versus* H_2O_2 treated group.

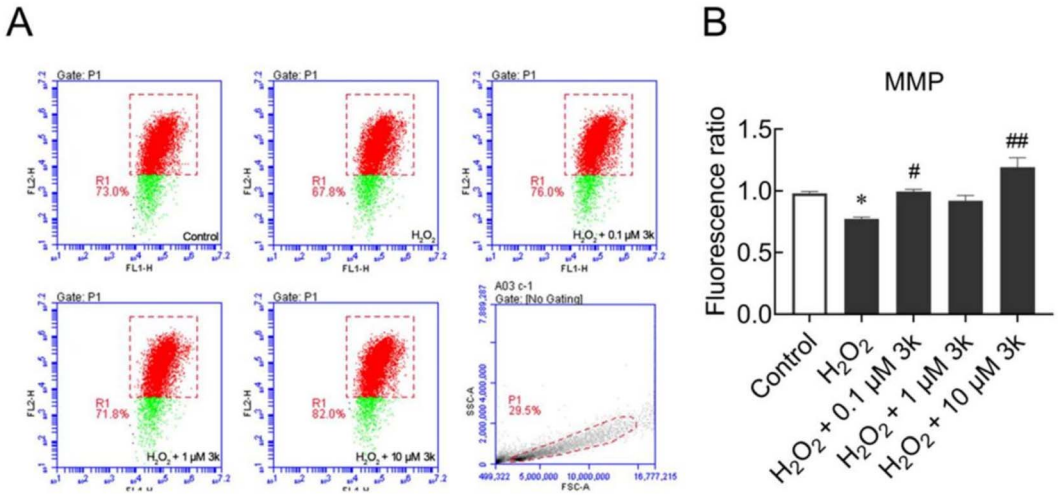

Fig. 3 **3k** prevented the decrease of MMP in H_2O_2-incubated SY5Y cells. (A) Variations of MMP with BD FACS Calibur flow cytometer detection using JC-1 probe. Red fluorescence represented higher MMP, while green fluorescence represented lower MMP. (B) Quantitative analysis of MMP in SY5Y cells. Error bars represent SEM. $^{\#}P < 0.05$, $^{\#\#}P < 0.01$ *versus* H_2O_2 treatment group, $^{*}P < 0.05$ *versus* control.

stress-induced cellular damage cells.[34–36] As shown in Fig. 2B, the levels of intracellular GSH were decreased after H_2O_2 stimulation, which was blocked by pretreatment with 10 μM of **3k**.

2.6. 3k prevented the injury of MMP induced by H_2O_2

Mitochondrial membrane potential (MMP) usually reflects the functional status of mitochondria, which was detected by the JC-1 fluorescent probe. As shown in Fig. 3A and B, the red fluorescence in SY5Y cells decreased significantly after 100 μM H_2O_2 treatment for 24 h. With 10 μM **3k** administration, the H_2O_2-induced reduction of MMP was blocked significantly. These findings indicated that **3k** can inhibit H_2O_2-mediated mitochondrial dysfunction.

2.7. *In vitro* blood–brain barrier permeation assay

To facilitate drugs' effectiveness in targeting the central nervous system, it is imperative that they possess commendable blood–brain-barrier (BBB) permeability. Di *et al.*[37] provided insights into this by assessing their compounds' BBB permeability using the Parallel Artificial Membrane Permeation Assay for the Blood–Brain-Barrier (PAMPA-BBB). To validate this, a comparative analysis was performed, measuring the experimental permeability of 9 commercially available drugs against previously documented values (Table 3). The results demonstrated a strong linear correlation between the experimental data and the bibliographic references, as expressed by the equation: Pe (exp.) = 1.033Pe (bibl.) + 0.2019 (R^2 = 0.9659) (Fig. 4). Leveraging this equation and taking into consideration Di *et al.*'s established threshold for BBB permeability, we have defined the subsequent permeability ranges: (a) 'CNS+' (high BBB permeation predicted): Pe ($\times 10^{-6}$ cm s^{-1}) > 4.33. (b) 'CNS−' (low BBB permeation predicted): Pe ($\times 10^{-6}$ cm s^{-1}) < 2.27. (c) 'CNS±' (BBB permeation uncertain): Pe ($\times 10^{-6}$ cm s^{-1}) from 4.33 to 2.27. From Table 4, the Pe values of all selective compounds were higher than 4.33, which indicated all compounds had a high permeability of the blood–brain barrier.

Table 3 Permeability Pe ($\times 10^{-6}$ cm s^{-1}) in the PAMPA-BBB assay for 9 commercial drugs in the experiment validation

Commercial drugs	Bibliography[a]	Experiment[b]
Testosterone	17.0	16.40 ± 0.47
Estradiol	12.0	13.20 ± 0.51
Progesterone	9.3	8.90 ± 0.34
Chlorpromazine	6.5	7.30 ± 0.85
Corticosterone	5.1	4.72 ± 0.59
Hydrocortisone	1.9	1.0 ± 0.23
Caffeine	1.3	0.79 ± 0.10
Atenolol	1.02	1.90 ± 0.21
Theophylline	0.1	0.54 ± 0.13

[a] Taken from ref. 37. [b] Experimental data are presented as mean from three independent experiments, using PBS : EtOH (70 : 30) as solvent.

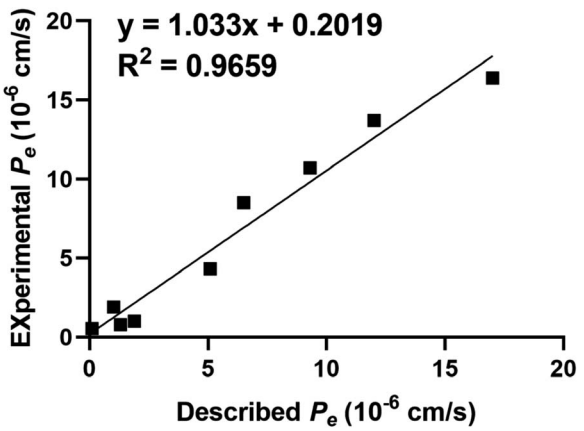

Fig. 4 Lineal correlation between experimental and reported permeability of commercial drugs using the PAMPA-BBB assay. Pe (exp.) = 1.033Pe (bibl.) + 0.2019 (R^2 = 0.9659).

Table 4 Permeability Pe ($\times 10^{-6}$ cm s^{-1}) in the PAMPA-BBB assay for selected compounds and their predicted penetration into CNS

Compd	Pe[a] ($\times 10^{-6}$ cm s^{-1})	Prediction[b]
3b	5.96 ± 0.78	CNS+
3c	8.45 ± 0.57	CNS+
3e	10.75 ± 1.03	CNS+
3f	6.24 ± 0.98	CNS+
3g	11.25 ± 0.68	CNS+
3h	7.68 ± 0.47	CNS+
3k	9.23 ± 0.57	CNS+
3m	10.58 ± 0.38	CNS+
3n	10.11 ± 0.34	CNS+
3q	6.54 ± 0.81	CNS+

[a] Permeability Pe ($\times 10^{-6}$ cm s^{-1}) values are presented as mean from three independent experiments, using PBS : EtOH (70 : 30) as solvent. [b] CNS+ is predicted as high BBB permeation with Pe ($\times 10^{-6}$ cm s^{-1}) > 4.33, CNS− is predicted as low BBB permeation with Pe ($\times 10^{-6}$ cm s^{-1}) < 2.27, CNS± is uncertain for BBB permeation with 2.27 < Pe ($\times 10^{-6}$ cm s^{-1}) < 4.33.

3. Conclusions

A series of capsaicin analogues **3a–3q** were designed, synthesized, evaluated their antioxidant activity and explored underlying neuroprotective mechanisms. The radical scavenging capacity of compound **3c–3q** was measured by DPPH and ABTS tests, respectively. Some analogues showed stronger antioxidant activity than the positive drug quercetin ($IC_{50} = 8.70 \pm 1.75$ μM for DPPH assay and 13.85 ± 2.87 μM for ABTS assay, respectively). According to the structure–activity relationship study, the phenolic hydroxyl of capsaicin analogues played a critical role in antioxidant activity. Compound **3k** had the best antioxidant activity in the ABTS assay among these compounds. Cytotoxicity assay showed that compound **3k** had little toxicity against the SH-SY5Y cell line. The promising compound **3k** had a significant protective effect on SH-SY5Y cells from oxidative damage induced by H_2O_2. Moreover, the determination of intercellular ROS and GSH levels further proved that compound **3k** not only prevented oxidative stress induced by H_2O_2 but also had neuroprotective effect on cells. In the mitochondrial membrane potential assay, the levels of MMP in H_2O_2-treated SH-SY5Y cells were increased significantly after a low concentration of **3k** incubation, indicating that mitochondrial function had been restored to a certain extent, which was beneficial for neurodegenerative diseases.

In summary, the objective of our study was to explore some potential antioxidant and neuroprotective agents and their possible mechanisms. The results from this paper not only help us to make better use of natural active ingredients but also provide more possibilities for the treatment of neurodegenerative disorder.

4. Experimental

4.1. Chemical reagents and instruments

Chemicals reagents were purchased at the highest commercial quality (>95%) and used without further purification. Reactions were monitored by thin-layer chromatography (TLC) carried out on 0.25 mm Tsingdao silica gel glass-backed plates and visualized under UV light at 254 nm. Tsingdao silica gel (particle size 0.040–0.063 mm) was used for flash column chromatography. Yields refer to chromatographically. The synthesized intermediates or target compounds were characterized by melting points apparatus, ^{1}H NMR, ^{13}C NMR and high-resolution mass spectrometry (HRESIMS) respectively, NMR spectra were obtained at 500 MHz (^{1}H) and 125 MHz (^{13}C) using Brüker Avance 500 spectrometer. Residual solvent peaks of DMSO-d_6 (δ H: 2.50 ppm, δ C: 39.52 ppm) and $CDCl_3$ (δ H: 7.26 ppm, δ C: 77.16 ppm) were used as an internal reference.

4.2. General procedure for the synthesis of compounds 3b–3q

To a solution of capsaicin **3a** (0.5 mmol, 1.0 equiv.) in dry THF (4 mL) was added Pd/C (10%), stirred at r.t. for 24 h under the H_2 atmosphere. After completion, the reaction mixture was filtered, concentrated and purified by flash chromatography on silica gel (eluent: PE/EtOAc, 10/1 to 1/1) to give compound **3b**.

To a solution of acid **2** (4.0 mmol, 1.0 equiv.) in DCM (25 mL) was added amine **1** (4.0 mmol, 1.0 equiv.), followed by HOBT (5.2 mmol, 1.3 equiv.), EDCI (5.2 mmol, 1.3 equiv.) and stirred at r.t. for 8 h. After completion, the reaction mixture was transferred to a 100 mL separating funnel, the additional 10 mL DCM was added, washed sequentially with H_2O (40 mL), 1 M HCl (40 mL) and saturated $NaHCO_3$ (40 mL). Repeated the above extraction procedure three times, the combined organic phases were washed with brine, dried by anhydrous Na_2SO_4, filtered and concentrated. Finally, the residue was purified by flash chromatography on silica gel (eluent: PE/EtOAc, 10/1 to 1/1) to give compounds **3d–3g**, **3i–3j**, **3l–3m**, **3o–3p**.

To a solution of **3b**, **3f**, **3i**, **3l**, **3o** (2.0 mmol, 1.0 equiv.) in DCM (15 mL) was added BBr_3 (4.0 mmol, 2.0 equiv.) dropwise at −76 °C and stirred for 3 h, then warmed up to r.t. for 2 h, the reaction was quenched by 3 mL H_2O, and the reaction mixture was transferred to a 100 mL separating funnel, the additional 15 mL DCM and 30 mL H_2O was added, then extracted three times with DCM (3 × 30 mL), the combined organic phases were washed with brine, dried by anhydrous Na_2SO_4, filtered and concentrated. Finally, the residue was purified by flash chromatography on silica gel (eluent: PE/EtOAc, 10/1 to 1/1) to give compounds **3c**, **3h**, **3k**, **3n**, **3q**.

4.2.1 Dihydrocapsaicin (3b). Yield 78.5%; a white solid; m.p.: 62–64 °C; ^{1}H NMR (600 MHz, $CDCl_3$) δ 6.86 (d, $J = 8.0$ Hz, 1H), 6.80 (s, 1H), 6.76 (d, $J = 8.0$ Hz, 1H), 5.67 (brs, 1H), 5.65 (s, 1H), 4.35 (d, $J = 5.6$ Hz, 2H), 3.87 (s, 3H), 2.19 (t, $J = 7.6$ Hz, 2H), 1.68–1.60 (m, 4H), 1.50 (dt, $J = 13.3$, 6.6 Hz, 1H), 1.35–1.28 (m, 2H), 1.28–1.22 (m, 4H), 1.13 (dd, $J = 13.9$, 6.9 Hz, 2H), 0.85 (d, $J = 6.6$ Hz, 6H); ^{13}C NMR (150 MHz, $CDCl_3$) δ 173.1, 146.8, 145.2, 130.5, 120.9, 114.5, 110.8, 56.1, 43.7, 39.1, 37.0, 29.8, 29.5, 28.1, 27.4, 25.9, 22.8; HRMS (ESI): *m*/*z* calcd for $C_{18}H_{30}NO_3^+[M + H]^+$: 308.2220; found: 308.2223.

4.2.2 *N*-(3,4-Dihydroxybenzyl)-8-methylnonanamide (3c). Yield 63.5%; a white solid; m.p.: 94–95 °C; ^{1}H NMR (500 MHz, *d*-DMSO) δ 8.79 (s, 1H), 8.70 (s, 1H), 8.10 (t, $J = 5.8$ Hz, 1H), 6.63

(d, J = 8.0 Hz, 2H), 6.47 (dd, J = 8.0, 2.1 Hz, 1H), 4.06 (d, J = 5.9 Hz, 2H), 2.08 (t, J = 7.4 Hz, 2H), 1.54–1.46 (m, 3H), 1.23 (s, 6H), 1.13 (dd, J = 13.5, 6.6 Hz, 2H), 0.85 (s, 3H), 0.84 (s, 3H); ^{13}C NMR (125 MHz, *d*-DMSO) δ 171.7, 145.0, 144.0, 130.5, 118.1, 115.2, 114.9, 41.6, 38.4, 35.3, 29.0, 28.7, 27.3, 26.6, 25.3, 22.4; HRMS (ESI): m/z calcd for $C_{17}H_{28}NO_3^+[M+H]^+$: 294.2064; found: 294.2063.

4.2.3 2-(3,4-Dimethoxyphenyl)-*N*-octylacetamide (3d). Yield 78.2%; a light-yellow oil; ^{1}H NMR (500 MHz, $CDCl_3$) δ 6.85 (d, J = 8.0 Hz, 1H), 6.80 (d, J = 1.7 Hz, 1H), 6.75 (dd, J = 8.0, 1.7 Hz, 1H), 4.34 (d, J = 5.4 Hz, 2H), 3.86 (s, 3H), 2.24–2.15 (m, 2H), 1.69–1.59 (m, 2H), 1.34–1.25 (m, 6H), 0.87 (t, J = 6.8 Hz, 3H). ^{13}C NMR (125 MHz, $CDCl_3$) δ 173.1, 146.9, 145.3, 130.5, 120.9, 114.5, 110.9, 56.1, 43.7, 37.0, 31.7, 29.1, 25.9, 22.6, 14.1; HRMS (ESI): m/z calcd for $C_{15}H_{24}NO_3^+[M+H]^+$: 266.1751; found: 266.1752.

4.2.4 *N*-(3,4-Dimethoxybenzyl)heptanamide (3e). Yield 68.3%; a white solid; m.p.: 84–85 °C ^{1}H NMR (500 MHz, $CDCl_3$) δ 6.81 (s, 3H), 4.36 (d, J = 5.5 Hz, 2H), 3.86 (s, 6H), 2.20 (t, J = 7.6 Hz, 2H), 1.69–1.58 (m, 2H), 1.36–1.24 (m, 6H), 0.87 (t, J = 6.8 Hz, 3H); ^{13}C NMR (125 MHz, $CDCl_3$) δ 173.1, 149.3, 148.6, 131.2, 120.2, 111.4, 111.4, 56.1, 56.0, 43.6, 37.0, 31.7, 29.1, 25.9, 22.6, 14.1; HRMS (ESI): m/z calcd for $C_{16}H_{26}NO_3^+[M+H]^+$: 280.1907; found: 280.1911.

4.2.5 *N*-Hexyl-2-(4-hydroxy-3-methoxyphenyl)acetamide (3f). Yield 67.0%; a light-yellow oil; ^{1}H NMR (500 MHz, *d*-DMSO) δ 8.73 (s, 1H), 7.84 (t, J = 5.3 Hz, 1H), 6.82 (d, J = 1.6 Hz, 1H), 6.67 (d, J = 8.0 Hz, 1H), 6.62 (dd, J = 8.0, 1.7 Hz, 1H), 3.73 (s, 3H), 3.25 (s, 2H), 3.01 (dd, J = 12.8, 6.8 Hz, 2H), 1.44–1.32 (m, 2H), 1.29–1.17 (m, 6H), 0.84 (t, J = 6.8 Hz, 3H); ^{13}C NMR (125 MHz, *d*-DMSO) δ 170.3, 147.2, 145.0, 127.3, 121.1, 115.1, 113.1, 55.5, 42.1, 38.5, 30.9, 29.0, 26.0, 22.0, 13.8; HRMS (ESI): m/z calcd for $C_{15}H_{24}NO_3^+[M+H]^+$: 266.1751; found: 266.1756.

4.2.6 2-(3,4-Dimethoxyphenyl)-*N*-hexylacetamide (3g). Yield 83.1%; a white solid; m.p.: 57–58 °C; ^{1}H NMR (500 MHz, $CDCl_3$) δ 6.84 (d, J = 8.3 Hz, 1H), 6.80–6.75 (m, 2H), 3.87 (s, 3H), 3.87 (s, 3H), 3.50 (s, 2H), 3.19 (dd, J = 13.2, 6.9 Hz, 2H), 1.43–037 (m, 2H), 1.26–1.18 (m, 6H), 0.85 (t, J = 6.9 Hz, 3H); ^{13}C NMR (125 MHz, $CDCl_3$) δ 171.3, 149.5, 148.5, 127.6, 121.8, 112.7, 111.7, 56.1, 56.0, 43.6, 39.8 31.5, 29.5, 26.6, 22.6, 14.1; HRMS (ESI): m/z calcd for $C_{16}H_{26}NO_3^+[M+H]^+$: 280.1907; found: 280.1911.

4.2.7 2-(3,4-Dihydroxyphenyl)-*N*-hexylacetamide (3h). Yield 50.6%; a white solid; m.p.: 111–112 °C; ^{1}H NMR (500 MHz, *d*-DMSO) δ 8.73 (s, 1H), 8.63 (s, 1H), 7.80 (t, J = 5.4 Hz, 1H), 6.64 (d, J = 2.0 Hz, 1H), 6.61 (d, J = 8.0 Hz, 1H), 6.47 (dd, J = 8.0, 2.0 Hz, 1H), 3.17 (s, 2H), 3.00 (dd, J = 12.8, 6.8 Hz, 2H), 1.36 (dd, J = 13.8, 6.9 Hz, 2H), 1.25 (dd, J = 15.5, 7.6 Hz, 6H), 0.85 (t, J = 6.9 Hz, 3H); ^{13}C NMR (125 MHz, *d*-DMSO) δ 170.3, 144.8, 143.7, 127.3, 119.6, 116.3, 115.2, 41.9, 38.5, 30.9, 29.0 26.0, 22.0, 13.8; HRMS (ESI): m/z calcd for $C_{14}H_{22}NO_3^+[M+H]^+$: 252.1594; found: 252.1595.

4.2.8 *N*-(4-Hydroxy-3-methoxybenzyl) octanamide (3i). Yield 65.5%; a white oil; ^{1}H NMR (500 MHz, $CDCl_3$) δ 6.85 (d, J = 8.0 Hz, 1H), 6.79 (d, J = 1.8 Hz, 1H), 6.74 (dd, J = 8.0, 1.8 Hz, 1H), 4.33 (d, J = 5.5 Hz, 2H), 3.86 (s, 3H), 2.19 (t, J = 7.6 Hz, 2H), 1.71–1.58 (m, 2H), 1.30–1.25 (m, 8H), 0.86 (t, J = 7.0 Hz, 3H); ^{13}C NMR (125 MHz, $CDCl_3$) δ 173.1, 146.9, 145.3, 130.5, 120.9, 114.5, 110.9, 56.0, 43.7, 36.9, 31.8, 29.4, 29.1, 25.9, 22.7, 14.2; HRMS (ESI): m/z calcd for $C_{16}H_{26}NO_3^+[M+H]^+$: 280.1907; found: 280.1908.

4.2.9 *N*-(3,4-Dimethoxybenzyl)octanamide (3j). Yield 69.4%; a white solid; m.p.: 96–97 °C; ^{1}H NMR (500 MHz, $CDCl_3$) δ 6.80 (s, 3H), 4.36 (d, J = 5.5 Hz, 2H), 3.85 (s, 6H), 2.20 (t, J = 7.6 Hz, 2H), 1.73–1.55 (m, 2H), 1.37–1.19 (m, 8H), 0.86 (t, J = 6.9 Hz, 3H); ^{13}C NMR (125 MHz, $CDCl_3$) δ 173.1, 149.3, 148.6, 131.2, 120.2, 111.4, 111.4, 56.1, 56.0, 43.5, 36.9, 31.8, 29.4, 29.1, 25.9, 22.7, 14.2; HRMS (ESI): m/z calcd for $C_{17}H_{28}NO_3^+[M+H]^+$: 294.2064; found: 294.2064.

4.2.10 *N*-(3,4-Dihydroxybenzyl)octanamide (3k). Yield 63.4%; a white solid; m.p.: 102–103 °C; ^{1}H NMR (500 MHz, *d*-DMSO) δ 8.73 (brs, 2H), 8.09 (t, J = 5.7 Hz, 1H), 6.63 (d, J = 8.1 Hz, 2H), 6.47 (dd, J = 8.0, 2.0 Hz, 1H), 4.06 (d, J = 5.9 Hz, 2H), 2.08 (t, J = 7.4 Hz, 2H), 1.58–1.44 (m, 2H), 1.34–1.16 (m, 8H), 0.86 (t, J = 6.9 Hz, 3H); ^{13}C NMR (125 MHz, *d*-DMSO) δ 171.8, 145.0, 144.0, 130.5, 118.1, 115.2, 114.9, 41.6, 35.3, 31.1, 28.6, 28.4, 25.3, 22.0, 13.9; HRMS (ESI): m/z calcd for $C_{15}H_{24}NO_3^+[M+H]^+$: 266.1751; found: 266.1749.

4.2.11 *N*-(4-Hydroxy-3-methoxybenzyl)nonanamide (3l). Yield 70.6%; a light-yellow oil; ^{1}H NMR (500 MHz, *d*-DMSO) δ 8.78 (s, 1H), 8.14 (t, J = 5.7 Hz, 1H), 6.80 (d, J = 1.7 Hz, 1H), 6.69 (d, J = 8.0 Hz, 1H), 6.63 (dd, J = 8.0, 1.8 Hz, 1H), 4.14 (d, J = 5.9 Hz, 2H), 3.73 (s, 3H), 2.10 (t, J = 7.4 Hz, 2H), 1.59–1.45 (m, 2H), 1.29–1.19 (m, 10H), 0.86 (t, J = 7.0 Hz, 3H); ^{13}C NMR (125 MHz, *d*-DMSO) δ 171.9, 147.4, 145.3, 130.5, 119.6, 115.1, 111.6, 55.5, 41.8, 35.3, 31.2, 28.7, 28.6, 28.6, 25.3, 22.0, 13.9; HRMS (ESI): m/z calcd for $C_{17}H_{28}NO_3^+[M+H]^+$: 294.2064; found: 294.2064.

4.2.12 *N*-(3,4-Dimethoxybenzyl)nonanamide (3m). Yield 66.0%; a white solid; m.p.: 99–100 °C; ^{1}H NMR (500 MHz, *d*-DMSO) δ 8.19 (t, J = 5.6 Hz, 1H), 6.87 (d, J = 8.2 Hz, 1H), 6.84 (d, J = 1.7 Hz, 1H), 6.75 (dd, J = 8.1, 1.8 Hz, 1H), 4.18 (d, J = 5.9 Hz, 2H), 3.72 (s, 3H), 3.72 (s, 3H), 2.11 (t, J = 7.4 Hz, 2H), 1.56–1.46 (m, 2H), 1.30–1.20 (m, 10H), 0.85 (t, J = 7.0 Hz, 3H); ^{13}C NMR (125 MHz, *d*-DMSO) δ 171.9, 148.6, 147.7, 132.2, 119.2, 111.7, 111.2, 55.5, 55.3, 41.7, 35.3, 31.2, 28.7, 28.6, 28.6, 25.3, 22.0, 13.9; HRMS (ESI): m/z calcd for $C_{18}H_{30}NO_3^+[M+H]^+$: 308.2220; found: 308.2214.

4.2.13 *N*-(3,4-Dihydroxybenzyl) nonanamide (3n). Yield 70.6%; a white solid; m.p.: 104–105 °C; ^{1}H NMR (500 MHz, *d*-DMSO) δ 8.78 (s, 1H), 8.69 (s, 1H), 8.09 (t, J = 5.7 Hz, 1H), 6.63 (d, J = 8.1 Hz, 2H), 6.47 (dd, J = 8.0, 2.0 Hz, 1H), 4.06 (d, J = 5.9 Hz, 2H), 2.08 (t, J = 7.4 Hz, 2H), 1.57–1.41 (m, 2H), 1.30–1.19 (m, 10H), 0.86 (t, J = 6.9 Hz, 3H); ^{13}C NMR (125 MHz, *d*-DMSO) δ 171.8, 145.0, 144.0, 130.5, 118.1, 115.2, 114.9, 41.6, 35.4, 31.2, 28.7, 28.7, 28.6, 25.3, 22.0, 13.9; HRMS (ESI): m/z calcd for $C_{16}H_{26}NO_3^+[M+H]^+$: 280.1907; found: 280.1907.

4.2.14 2-(4-Hydroxy-3-methoxyphenyl)-*N*-octylacetamide (3o). Yield 70.6%; a light-yellow oil; ^{1}H NMR (500 MHz, *d*-DMSO) δ 8.73 (s, 1H), 7.84 (t, J = 5.4 Hz, 1H), 6.82 (d, J = 1.7 Hz, 1H), 6.67 (d, J = 8.0 Hz, 1H), 6.62 (dd, J = 8.0, 1.8 Hz, 1H), 3.73 (s, 3H), 3.25 (s, 2H), 3.01 (dd, J = 12.8, 6.8 Hz, 2H), 1.44–1.31 (m, 2H), 1.27–1.20 (m, 10H), 0.85 (t, J = 7.0 Hz, 3H); ^{13}C NMR (125 MHz, *d*-DMSO) δ 170.3, 147.2, 145.0, 127.3, 121.1, 115.1, 113.1, 55.5, 42.1, 38.2, 31.2, 29.1, 28.7, 28.6, 26.3, 22.0, 13.9; HRMS

(ESI): *m*/*z* calcd for $C_{17}H_{28}NO_3^+[M + H]^+$: 294.2064; found: 294.2063.

4.2.15 2-(3,4-Dimethoxyphenyl)-*N*-octylacetamide (3p). Yield 78.2%; a white solid; m.p.: 76–77 °C; ^{1}H NMR (500 MHz, $CDCl_3$) δ 6.84 (d, J = 8.4 Hz, 1H), 6.79–6.75 (m, 2H), 3.87 (s, 3H), 3.87 (s, 3H), 3.51 (s, 2H), 3.19 (dd, J = 13.2, 6.9 Hz, 2H), 1.43–1.37 (m, 2H), 1.29–1.19 (m, 10H), 0.86 (t, J = 7.0 Hz, 3H); ^{13}C NMR (125 MHz, $CDCl_3$) δ 171.3, 149.5, 148.5, 127.6, 121.8, 112.6, 111.7, 56.1, 56.0, 43.6, 39.8, 31.9, 29.6, 29.3, 29.3, 26.9, 22.7, 14.2; HRMS (ESI): *m*/*z* calcd for $C_{18}H_{30}NO_3^+[M + H]^+$: 308.2220; found: 308.2223.

4.2.16 2-(3,4-Dihydroxyphenyl)-*N*-octylacetamide (3q). Yield 77.0%; a white solid; m.p.: 89–90 °C; ^{1}H NMR (500 MHz, *d*-DMSO) δ 8.73 (s, 1H), 8.63 (s, 1H), 7.80 (t, J = 5.4 Hz, 1H), 6.64 (d, J = 2.0 Hz, 1H), 6.61 (d, J = 8.0 Hz, 1H), 6.47 (dd, J = 8.0, 2.0 Hz, 1H), 3.16 (s, 2H), 3.00 (dd, J = 12.8, 6.8 Hz, 2H), 1.41–1.33 (m, 2H), 1.30–1.18 (m, 10H), 0.86 (t, J = 7.0 Hz, 3H); ^{13}C NMR (125 MHz, *d*-DMSO) δ 170.3, 144.8, 143.7, 127.3, 119.5, 116.3, 115.2, 41.9, 38.5, 31.2, 29.1, 28.7, 28.6, 26.3, 22.0, 13.9; HRMS (ESI): *m*/*z* calcd for $C_{16}H_{26}NO_3^+[M + H]^+$: 280.1907; found: 280.1909.

4.3. DPPH radical scavenging assay

According to the reported method,[29] antioxidant activities of compounds **3a–3q** were evaluated by determination of DPPH radical scavenging activity. Quercetin was used as a positive control for antioxidant activity. In sample terms, the concentration gradient of compounds was diluted with 0.2 mL methanol, and 2 mL DPPH solution (0.5 mM) was added. After 30 min, the absorbance of the compounds of each concentration at 517 nm was measured. The calculation formula of DPPH free radical scavenging rate is as follows: DPPH radical scavenging (%) = $[A_{DPPH} - A_{(DPPH + compound)}]/A_{DPPH} \times 100\%$. The radical scavenging activity is represented by the average $IC_{50} \pm$ SEM of the experiment repeated three times.

4.4. ABTS radical cationic decolorization assay

The antioxidant activity of the compounds can be determined according to the method reported in the literature.[38] As described below, solid manganese dioxide is added to 20 mL 5 mM ABTS solution preconfigured with 75 mM Na/K buffer of pH 7. Quercetin was used as a positive control for antioxidant activity, and its standard curve was determined at a series of different concentrations. The compounds were vortically, ultrasonically, centrifugally and extracted in methanol : water (1 : 1, v/v) solution, and diluted appropriately in a Na/K buffer of pH 7. The diluted sample was mixed with 200 μL of ABTS radical cationic solution in a 96-well plate and the absorbance at 750 nm is read in a ThermoMax micrometer. The sample was repeated three times. The results were calculated according to the standard curve.

4.5. Cell culture and treatment

Human neuroblastoma SH-SY5Y cells were purchased from Stem Cell Bank, Chinese Academy of Sciences. SH-SY5Y cells were maintained routinely in Minimum Essential Medium (Invitrogen, 11090081) and Ham's F-12 Nutrient Mixture (Invitrogen, 11765054) supplemented with 10% fetal bovine serum (Gibco), 1% Gluta-max (Invitrogen, 35050061), sodium pyruvate (Invitrogen, 11360070), NEAA (Invitrogen, 11140050) at 37 °C in a humidified atmosphere of 5% CO_2 and 95% air. The medium was changed every 2 days. Cells were exposed to 100 μM H_2O_2 (Sigma-Aldrich) in the presence or absence of **3k** in all experiments.

4.6. Analysis of cell viability using MTT assay

SH-SY5Y cells were plated into 96-well plates at a density of 8×10^3 cells per well for 24 h. The cytotoxicity of quercetin (control group), **3a**, **3b**, **3c**, **3k**, **3n** and **3q** (0, 5, 10, 20, 40 or 80 μM) were detected by MTT assay. SY5Y cells were incubated with quercetin (control group), **3a**, **3b** and **3k** (0.1, 1 or 10 μM) at 37 °C for 3 h, prior to the addition of H_2O_2 (100 μM) for 24 h. And then MTT was added for 4 h, the culture solution was removed and DMSO was added to dissolve the formazan. Using a microplate reader (Spectramax Plus 384, Molecular Devices, Sunnyvale, CA, USA) to detect the absorbance at 570 nm.

4.7. Measurement of intracellular reactive oxygen species

Intracellular reactive oxygen species (ROS) levels were examined by a Reactive Oxygen Species Assay Kit (Beyotime, China). SY5Y cells were treated with **3k** (0.1, 1 or 10 μM) for 3 h, prior to the addition of H_2O_2 (100 μM) for 24 h. Then the cells were incubated with 10 μM DCFH-DA at 37 °C for 20 min. In the end, the fluorescence of DCF (FITC) was detected using ImageXpress® Micro Confocal (Molecular Devices, USA).

4.8. Measurement of glutathione

SY5Y cells were treated with **3k** (0.1, 1 or 10 μM) for 3 h, prior to the addition of H_2O_2 (100 μM) for 24 h. Based on the instructions of the manufacturer (Beyotime, China), we used the DTNB [5,5′-dithiobis(2-nitrobenzoic acid)]-GSSG reductase recycling assay to examine total glutathione (GSH) levels at 412 nm, compared to control.

4.9. Mitochondrial membrane potential assay

JC-1 was used to detect mitochondrial membrane potential (MMP). When the MMP is high, in a normal state, JC-1 produces red fluorescence. While the MMP is low, JC-1 cannot collect in the matrix of mitochondria and produce green fluorescence.

A change in the fluorescence from red to green displays a decrease of in the MMP. After the treatment above, the cells were incubated with a JC-1 probe for 20 min at 37 °C based on the instructions of the manufacturer (Beyotime, China). Then, the fluorescence was tested through BD FACS Calibur flow cytometer (Becton & Dickinson Company, Franklin Lakes, NJ).

4.10. Statistical analysis

The Tukey multiple comparison test statistical method was used for experimental analysis by GraphPad Prism version 8.0.2 (GraphPad Software, San Diego, CA). $P < 0.05$ indicates

a significant difference. The data are shown as mean ± standard error of mean ($x \pm$ SEM).

4.11. *In vitro* blood–brain barrier permeation assay

The blood–brain-barrier (BBB) permeability of synthesized compounds was assessed using the Parallel Artificial Membrane Permeation Assay (PAMPA). The experimental materials included commercial drugs sourced from Sigma and Alfa Aesar, porcine brain lipid (PBL) from Avanti Polar Lipids, a donor microplate with a PVDF membrane (pore size 0.45 mm), an acceptor microplate, and a 96-well UV plate from Corning Incorporated. To prepare the assay, the filter membrane was coated with PBL (4 mL) in dodecane (20 mg mL^{-1}), and the acceptor 96-well microplate was treated with 300 mL of PBS/EtOH (7 : 3) solution. The compounds were diluted to a concentration of 100 mg mL^{-1} using a solution of DMSO (<0.1%) and PBS/EtOH (7 : 3) and then added to the donor wells. A sandwich was created by placing the donor and acceptor filter membranes together, and this assembly was left undisturbed for 16 hours at 25 °C. The concentration of the compound in the acceptor wells was measured using a UV-plate reader (FlexStation® 3). Commercial drugs with known BBB permeability were included as controls in this experiment.

Author contributions

M. X., Z. Y.: conceptualization; M. X., H. W., J. B.: methodology; M. X.: funding acquisition; M. X., Z. Y., J. B.: project administration; M. X., Z. Y., J. B.: supervision; S. H., Y. X., Y. Q.: formal analysis; H. W.: writing – original draft; M. X., H. W., J. B., S. H., Y. X., Y. Q., Z. Y.: writing – review & editing. All authors contributed to the article and approved the submitted version.

Conflicts of interest

The authors declare no conflict of interest.

Acknowledgements

This work is supported by the Guangxi Natural Science Foundation for Youth Science Foundation (No. 2022GXNSFBA035478), the Guangxi Science and Technology Base and Talent Special Project (Grant No. AD21220076), the Guangxi Natural Science Foundation for Youth Science Foundation (No. 2023GXNSFBA026321), the State Key Laboratory for Chemistry and Molecular Engineering of Medicinal Resources (Guangxi Normal University, CMEMR2023-B10), the Guangxi Medical University Training Program for Distinguished Young Scholars.

References

1 S. A. Pal and P. Bigoniya, *Research & Reviews: A Journal of Pharmacognosy*, 2018, **5**, 25–38.
2 X.-J. Luo, J. Peng and Y.-J. Li, *Eur. J. Pharmacol.*, 2011, **650**, 1–7.
3 P. Patowary, M. P. Pathak, K. Zaman, *et al.*, *Biomed. Pharmacother.*, 2017, **96**, 1501–1512.
4 G. Jia, S. Cang, P. Ma, *et al.*, *Bioorg. Chem.*, 2020, **103**, 104161.
5 F. Aiello, M. Badolato, F. Pessina, *et al.*, *ACS Chem. Neurosci.*, 2016, **7**, 737–748.
6 K. Kogure, *Biochim. Biophys. Acta*, 2002, **1573**, 84–92.
7 Y. Okada, K. Tanaka, E. Sato, *et al.*, *J. Am. Oil Chem. Soc.*, 2010, **87**, 1397–1405.
8 Z. C. Wang, B. Wei, F. N. Pei, *et al.*, *Eur. J. Med. Chem.*, 2020, **198**, 112352.
9 F. Naaz, A. Khan, A. Kumari, *et al.*, *Bioorg. Chem.*, 2021, **113**, 105031.
10 E. Viayna, N. Coquelle, M. Cieslikiewicz-Bouet, *et al.*, *J. Med. Chem.*, 2021, **64**, 812–839.
11 M. Homayouni-Tabrizi, A. Asoodeh and M. Soltani, *J. Food Drug Anal.*, 2017, **25**, 567–575.
12 A. Capperucci, M. Coronnello, F. Salvini, *et al.*, *Bioorg. Chem.*, 2021, **110**, 104812.
13 G. J. Burton and E. Jauniaux, *Best Pract. Res. Clin. Obstet. Gynaecol.*, 2011, **25**, 287–299.
14 C. C. Winterbourn, *Nat. Chem. Biol.*, 2008, **4**, 278–286.
15 T. Persson, B. O. Popescu and A. Cedazo-Minguez, *Oxid. Med. Cell. Longevity*, 2014, **2014**, 427318.
16 K. Sugamura and J. F. Keaney Jr, *Free Radical Biol. Med.*, 2011, **51**, 978–992.
17 C. Wen, J. Zhang, Y. Feng, *et al.*, *Food Chem.*, 2020, **327**, 127059.
18 A. Spector, *J. Ocul. Pharmacol. Ther.*, 2000, **16**, 193–201.
19 I. Liguori, G. Russo, F. Curcio, *et al.*, *Clin. Interventions Aging*, 2018, **13**, 757–772.
20 P. Sooknual, R. Pingaew, K. Phopin, *et al.*, *Bioorg. Chem.*, 2020, **105**, 104384.
21 Y. Bai, D. Liu, H. Zhang, *et al.*, *Bioorg. Chem.*, 2021, **115**, 105255.
22 S. Shi, H. Wang, J. Wang, *et al.*, *Bioorg. Chem.*, 2020, **100**, 103917.
23 M. T. Lin and M. F. Beal, *Nature*, 2006, **443**, 787–795.
24 A. Dairam, R. Fogel, S. Daya, *et al.*, *J. Agric. Food Chem.*, 2008, **56**, 3350–3356.
25 Q. A. Nazari, T. Kume, N. Izuo, *et al.*, *Biol. Pharm. Bull.*, 2013, **36**, 1356–1362.
26 P. Bakthavachalam and P. S. T. Shanmugam, *J. Neurol. Sci.*, 2017, **375**, 417–423.
27 T. Iijima, *Neurosci. Res.*, 2006, **55**, 234–243.
28 W. M. Pardridge, *Alzheimer's Dementia*, 2009, **5**, 427–432.
29 M. N. Alam, N. J. Bristi and M. Rafiquzzaman, *Saudi Pharm. J.*, 2013, **21**, 143–152.
30 V. Dias, E. Junn and M. M. Mouradian, *J. Parkinson's Dis.*, 2013, **3**, 461–491.
31 A. Singh, R. Kukreti, L. Saso, *et al.*, *Molecules*, 2019, **24**, 1583.
32 K. J. Barnham, C. L. Masters and A. I. Bush, *Nat. Rev. Drug Discovery*, 2004, **3**, 205–214.
33 M. A. Martinez, J. L. Rodriguez, B. Lopez-Torres, *et al.*, *Environ. Int.*, 2020, **135**, 105414.
34 M. Jozefczak, T. Remans, J. Vangronsveld, *et al.*, *Int. J. Mol. Sci.*, 2012, **13**, 3145–3175.

35 P. Diaz-Vivancos, A. de Simone, G. Kiddle, *et al.*, *Free Radical Biol. Med.*, 2015, **89**, 1154–1164.
36 T. Homma and J. Fujii, *Curr. Drug Metab.*, 2015, **16**, 560–571.
37 L. Di, E. H. Kerns, K. Fan, *et al.*, *Eur. J. Med. Chem.*, 2003, **38**, 223–232.
38 N. P. Seeram, S. M. Henning, Y. Niu, *et al.*, *J. Agric. Food Chem.*, 2006, **54**, 1599–1603.